

Recent Advances in Magnetic Tweezers

Iwijn De Vlaminck and Cees Dekker

Kavli Institute of Nanoscience, Delft University of Technology, Delft, 2628 CJ,
The Netherlands; email: c.dekker@tudelft.nl

Annu. Rev. Biophys. 2012. 41:453–72

First published online as a Review in Advance on
March 14, 2012

The *Annual Review of Biophysics* is online at
biophys.annualreviews.org

This article's doi:
[10.1146/annurev-biophys-122311-100544](https://doi.org/10.1146/annurev-biophys-122311-100544)

Copyright © 2012 by Annual Reviews.
All rights reserved

1936-122X/12/0609-0453\$20.00

Keywords

magnetic tweezers instrumentation, highly multiplexed magnetic tweezers,
hybrid instruments, torque-sensitive magnetic tweezers

Abstract

Since their first demonstration of manipulation and mechanical coiling of a single DNA molecule, magnetic tweezers have become a popular and widely used single-molecule manipulation technique. Magnetic tweezers have yielded a wealth of information on the elastic properties of (coiled) DNA and have provided critical insights into the dynamic activity of DNA-processing enzymes. Recent years have seen a wave of technological creativity, and a flurry of new methods and technological advances have been introduced to magnetic tweezers, which will enable more and previously inaccessible information to be extracted from biophysical systems. In this review, we survey the most important recent advances and reflect on more interesting twists to come.

Contents

INTRODUCTION	454
FUNDAMENTALS	455
TOWARD HIGH-RESOLUTION MAGNETIC TWEEZERS	457
Resolution Limits	457
Camera-Based Position Tracking	458
Future Prospects	459
FROM SINGLE-MOLECULE TO KILO-MOLECULE	
MAGNETIC TWEEZERS	460
See More Beads	461
Stretch More Molecules	461
More Is More	462
MEASUREMENTS OF TORQUE	462
HYBRID INSTRUMENTS	464
Magnetic Tweezers Meet Optical Tweezers	464
Combinations with Fluorescence Microscopy	466
CONCLUSIONS AND OUTLOOK	466

INTRODUCTION

In demonstrations of the phenomenon of magnetism, iron filings dispersed on a piece of paper that is held close to a magnet orient and align to reveal the distribution of magnetic field lines produced by the magnet and faithfully follow the magnet's movements and rotations. Following the same principles, Crick & Hughes (21) used magnetic actuation of motion to drag, twist, and prod magnetic particles within the cytoplasm of cells, thereby providing the first demonstration of magnetic tweezers. Smith et al., and later Strick et al., performed a beautiful series of experiments in which they used magnetic actuation to stretch (82) and coil (85) an individual molecule of DNA tethered between a flow cell surface and a microscopic magnetic particle. These authors laid the groundwork for a single-molecule manipulation technique that is now widely used and known as single-molecule magnetic tweezers.

In single-molecule magnetic tweezers, the magnetic particles of choice are micron-sized superparamagnetic beads. An individual double-stranded DNA (dsDNA) (55, 99), a single-stranded DNA (ssDNA) (97), a dsRNA (2), a DNA hairpin (44, 64), a DNA Holliday junction (25, 56), or a nucleosome fiber (51) can be tethered between the surface of a flow cell and the paramagnetic bead. The molecule is stretched and coiled by positioning and rotation of an external magnet, respectively (4, 84). The end-to-end distance of the molecule is measured by extracting the x , y , and z positions of the bead using video microscopy. The basic implementation of magnetic tweezers has provided scientists with detailed insight into the elastic properties of (coiled) DNA (5, 13, 14, 69, 86, 88) and has deepened our understanding of the dynamic activity of polymerases (63, 78), helicases (28, 64), topoisomerases (47, 49), recombinases (8, 94, 95, 97), and DNA-binding proteins (27, 102). The popularity of magnetic tweezers is due mainly to the low cost and simplicity of its implementation, as well as the possibility of directly investigating the effect of torque and twist on the dynamics of biomolecular interactions. DNA-enzyme interactions are often sensitive to torque applied to the DNA, particularly when the reaction is accompanied by a change in DNA topology, and structural and kinetic insight into the reaction can be obtained in these cases from

torque spectroscopy studies (27, 47). Moreover, torque plays a regulatory role in many aspects of cellular biology, for example, in reactions at the heart of transcription, replication, and recombination (27, 48, 52, 93), and the cell has intricate machinery in place to regulate supercoiling of cellular DNA (48). Magnetic tweezers are thus a powerful tool to address questions related to a wide range of biological systems.

Next to these beneficial attributes, the basic implementation of magnetic tweezers also entails a number of limitations. First, to date, the camera-based detection used in magnetic tweezers has limited the temporal and spatial resolution in measurements. Gathering structural information with the level of detail accessible in, for example, optical-tweezers-based assays (1, 67) has therefore proved difficult so far. Second, the enzyme activity on DNA is typically inferred from measurements of the length of the molecule, an indirect measurement in which information about the location of the enzyme interaction along the DNA is lost. In contrast to, for example, fluorescence-based measurements (42), the length-based measurement approach used in magnetic tweezers restricts their use to the study of relatively strong DNA-enzyme interactions that give rise to measurable changes in length (4). Third, magnetic tweezers allow straightforward application of torque, but the torque applied to the molecule is weak, typically orders of magnitude weaker than the torque exerted on the bead through the applied magnetic field. As a result, direct measurements of the applied torque from, e.g., changes in the equilibrium angle of the bead, are not readily possible. Last, as is the case for most single-molecule manipulation techniques (73), only a single molecule is addressed in a typical magnetic tweezers assay, leading to a low experimental throughput.

In recent years these limitations have been addressed, and a number of methods have been introduced that significantly expand the parameter space that is accessible with magnetic tweezers. Here, we discuss the most important of these recent advances in technology and instrumentation and we outline various future applications. The topics discussed include recent efforts directed toward increasing the experimental throughput in magnetic tweezers via multiplexing, improvements in the resolution of magnetic-tweezers-based measurements, recent developments of torque-sensitive magnetic tweezers, combinations of magnetic tweezers with fluorescence-based measurements, and combinations of magnetic tweezers with other single-molecule manipulation techniques. Finally, we speculate on technological developments that can be expected in the near future.

Optical tweezers:
method to trap and
manipulate an object
with a tightly focused
laser beam

FUNDAMENTALS

As the instrumentation used in magnetic tweezers and the physical principles that underlie the technique have been described in detail elsewhere (64, 72, 73, 84, 99), we restrict ourselves to a brief overview of the most important aspects. **Figure 1** outlines the canonical implementation of magnetic tweezers. A magnet is positioned above a flow cell that is placed on an inverted microscope. The magnetic force field is usually generated with a pair of permanent magnets, but implementations based on electromagnets (29, 34, 37) or the near-field of a single permanent magnet (103) have also been reported. The applied magnetic field induces a magnetic moment in the paramagnetic bead and the bead experiences a force proportional to the gradient of this field. Forces between 10 and 100 pN can be readily exerted on paramagnetic beads with diameter of 1 to 3 μm (46, 58) by using magnets that are conveniently positioned outside of the flow chamber. The characteristic length scale over which the magnetic field gradient varies is large, typically on the order of 1 mm. As a result, the generated force can at good approximation be assumed constant over the length scale that a tethered bead moves. Magnetic tweezers thus provide an infinite bandwidth force clamp without the necessity of sophisticated active force feedback required with optical tweezers (73).

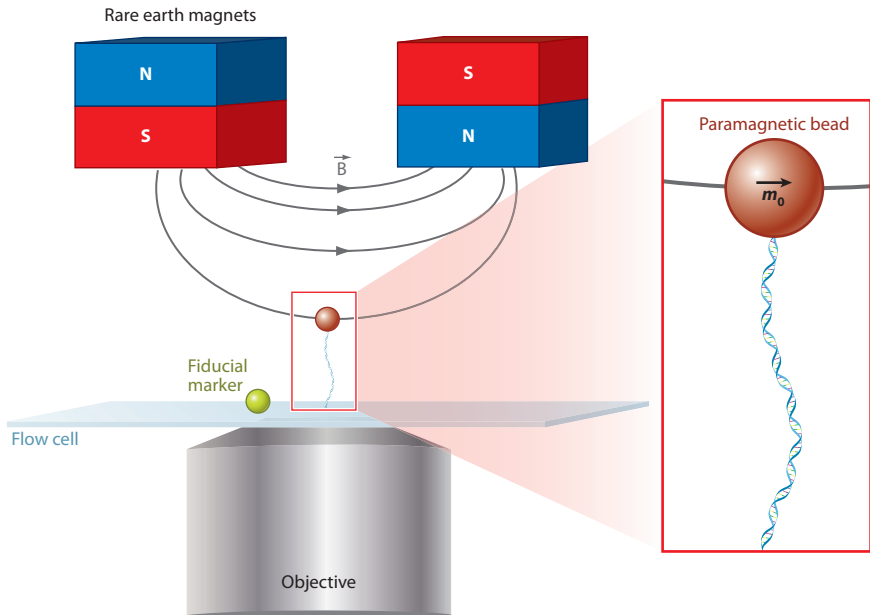


Figure 1

Schematic of basic implementation of magnetic tweezers. A molecule is tethered between the surface of a flow cell and a paramagnetic bead. The magnetic field generated by a pair of magnets induces a magnetic moment m_0 in the paramagnetic bead. The bead experiences a force proportional to the gradient of the field. The molecule can be coiled by rotating the external magnet. Abbreviations: N, magnetic north pole; S, magnetic south pole.

In the presence of an applied field, the paramagnetic beads commonly employed in magnetic tweezers rotate and align to the applied magnetic field. This is explained by either a small permanent magnetic component in the beads or an easy axis in the paramagnetic polarizability of the beads. The resulting torque exerted on the paramagnetic beads is strong, typically on the order of 10^4 to 10^5 pN nm rad $^{-1}$ (45, 60), which allows rapid rotation of the beads in the presence of a rotating magnetic field (20, 41). This property is exploited in magnetic tweezers to coil and torsionally strain the tethered molecule.

The magnetic bead acts simultaneously as force transducer and position probe. Position measurements in magnetic tweezers are performed using video microscopy. The xy position of the bead is first determined either by direct fitting of the subpixel location of the bead (center-of-mass techniques or Gaussian fitting of the intensity profile) (12) or by image-reference (a mirror image, a previous image, or a predefined kernel) cross-correlation (31, 34). A quantitative comparison of these tracking algorithms showed that two-dimensional image-reference cross-correlation is the most accurate and robust tracking method (18). To extract the bead height or z position, which is a measure for the DNA end-to-end distance, a lookup table of images of the diffraction pattern of the bead is generated before the experiment that links the bead height to the shape and size of the diffraction pattern (34). During the experiment, the diffraction pattern of the bead is compared in real time to the lookup table images and the bead height is extracted after fitting (99). The vertical force applied to the magnetic bead is calibrated by analyzing the spectrum of the thermal fluctuations of the bead (85). The effects of finite integration time (101) and finite bandwidth of

the camera must be appropriately corrected for (90). These corrections become increasingly more important at higher applied forces, for shorter molecules, and for smaller beads (99).

Slow sample drift is accounted for by measuring the position of the bead with reference to one or several nonmagnetic fiducial markers that are fixed to the flow cell surface (85, 88). Given the weak dependence of the applied force on bead position in x , y , and z , drift in the sample or magnet position does not give rise to appreciable changes in the applied force, removing the necessity of a complex feedback system. Furthermore, magnetic tweezers do not require complex designs to cope with additional, instrument-dependent sources of noise such as those found in optical tweezers: laser pointing instability, acoustic noise, and laser noise (67). Here lies an important advantage of magnetic tweezers over alternative single-molecule manipulation techniques: Magnetic tweezers are in general insensitive to low-frequency noise (<1 Hz) and inherently provide ultrastable operation.

TOWARD HIGH-RESOLUTION MAGNETIC TWEEZERS

Despite the insensitivity of magnetic tweezers to sources of low-frequency noise and drift, sub-nanometer measurements of biological activity have to date not been demonstrated with magnetic tweezers. This is due to the limited resolution of camera-based position measurements, which has long been the Achilles' heel of magnetic tweezers. Recent technical advances and ongoing developments in camera and computer hardware, however, will likely change this situation in the near future. Before we describe these recent trends and future prospects, we discuss the various sources of noise that limit the measurement resolution.

Resolution Limits

The position resolution in magnetic tweezers is limited by both the intrinsic thermal fluctuations of the bead and the instrument-dependent resolution in position tracking. Let us first consider the intrinsic fluctuations of the bead height, as these set the ultimate resolution attainable for length measurements. The bead experiences a frequency-independent (white) thermal force from the aqueous environment with noise spectral density $S_F(f) = 4\gamma k_B T$, where γ is the hydrodynamic drag coefficient, T is the temperature, and k_B is the Boltzmann constant. The thermal force noise gives rise to the following power spectral density of the bead height (32):

$$S_z(f) = \frac{k_b T}{\gamma \pi^2 (f_c^2 + f^2)}, \quad 1.$$

where $f_c = \kappa_{tether}/2\pi\gamma$ is the mechanical response frequency of the DNA-bead tether, and κ_{tether} is the length- and force-dependent stiffness of the molecule. The smallest detectable change in bead height, considering only thermal force noise, then is $\delta z_{thermal} = std(z)SNR$, where SNR is the desired signal-to-noise ratio and $std(z)$ is the standard deviation in bead height fluctuations. $std(z)$ can be computed by integrating the power spectral density of the bead fluctuations over the relevant measurement bandwidth. For $SNR = 1$, δz reads

$$\delta z_{thermal} = \left[\int_0^{B_{eq}} S_z(f) df \right]^{\frac{1}{2}} = \left[\frac{2k_b T}{\pi \kappa_{tether}} \arctan \left(\frac{B_{eq}}{f_c} \right) \right]^{\frac{1}{2}}, \quad 2.$$

where we define B_{eq} as the equivalent noise bandwidth, i.e., the bandwidth of a fictitious rectangular low-pass filter that gives rise to the same noise power as the actual measurement system. B_{eq} represents the effects of the finite shutter time and frame rate of the camera (90, 101), but it also accounts for potential smoothing filters applied by the experimentalist after data acquisition. For an

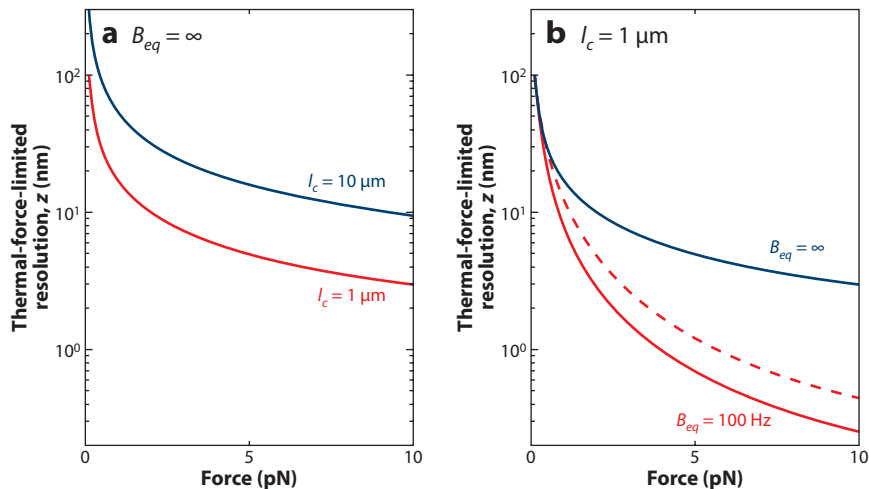


Figure 2

Thermal-force-limited position resolution in magnetic tweezers. Smallest detectable displacement in z direction, $\delta z_{thermal}$, with signal-to-noise-ratio = 1, considering thermal fluctuations in bead height (see Equation 2). $\delta z_{thermal} = [\frac{2k_b T}{\pi \kappa_{tether}} \arctan(\frac{B_{eq}}{f_c})]^{\frac{1}{2}}$, where κ_{tether} is the force-dependent stiffness of the molecule and B_{eq} is the equivalent noise bandwidth. (a) $\delta z_{thermal}$ is plotted as a function of applied force for noncoiled double-stranded DNA molecules with different contour lengths, $l_c = 1 \mu\text{m}$ (red line) and $l_c = 10 \mu\text{m}$ (blue line), for the case in which the bead fluctuations are measured with an infinite bandwidth, $B_{eq} = \infty$. (b) $\delta z_{thermal}$ as a function of force for a molecule with $l_c = 1 \mu\text{m}$ tethered to magnetic beads of different size, bead diameter = 1 μm (solid lines) and 3 μm (dashed lines) and for different measurement bandwidth, $B_{eq} = \infty$ (blue line and markers) and $B_{eq} = 100 \text{ Hz}$ (red lines and markers). For $B_{eq} = \infty$, δz is independent of bead size, and the dashed and solid lines overlap. In the model, κ_{tether} is derived from the seven-parameter analytical approximation to the worm-like-chain force response of double-stranded DNA as proposed by Bouchiat et al. (11).

infinite bandwidth system, $\delta z_{thermal}$ simply reads $\sqrt{k_b T / \kappa_{tether}}$, in accordance with the equipartition theorem. For $B_{eq} \ll f_c$, $\delta z_{thermal} \sim \sqrt{B_{eq}}$, and a trade-off thus exists between the measurement time resolution and position resolution. The thermal-force-limited resolution is dependent on the tether length and applied force, with higher forces and shorter tethers leading to a higher resolution (66). **Figure 2a,b** plots the thermal-force-limited resolution as a function of the applied force for noncoiled dsDNA molecules with different lengths ($l_c = 1 \mu\text{m}$ and $l_c = 10 \mu\text{m}$) and for equivalent bandwidths $B_{eq} = 100 \text{ Hz}$, and $B_{eq} = \infty$. Here, κ_{tether} is calculated on the basis of the seven-parameter analytical approximation to the worm-like-chain force response of dsDNA as proposed by Bouchiat et al. (11). As is clear from the graph, subnanometer resolution can be obtained for a measurement system with $B_{eq} = 100 \text{ Hz}$ and a tether length of 1 μm under an applied force $> 3 \text{ pN}$.

Camera-Based Position Tracking

Although Equation 2 accounts for the influence of the frequency response of the video microscopy system on the thermal-force-limited resolution, it disregards the additional noise introduced by video-based tracking. In the standard implementation of magnetic tweezers, the length of the molecule is inferred from measurements of the bead position along the z -axis, typically the axis of illumination of the imaging system for which the tracking resolution is typically a factor

5–10 lower than the resolution in the x or y directions. The precision of position determination based on a camera image can be improved by increasing the number of pixels comprising the image, N_{pixel} , or by increasing the rate of image acquisition, f_r . The smallest displacement that can be detected assuming camera noise only, δz_{camera} , scales as

$$\delta z_{camera} \sim \sqrt{\frac{1}{N_{pixel} f_r}}. \quad 3.$$

CMOS camera:
complementary metal-oxide-semiconductor
image sensor array

Future Prospects

Because of limitations in the resolution of video-microscopy-based tracking of the bead height [$\delta z_{camera} = 10$ nm for the early demonstration by Strick et al. (87)], the observation of enzyme dynamics with subnanometer precision, as demonstrated for optical tweezers (1, 19), is a yet-to-be achieved goal for magnetic tweezers. There is, however, good hope that such high-resolution magnetic tweezers will become available in the near future.

First, ongoing developments in camera technology make cameras with smaller pixels and faster acquisition rates available to researchers and allow further improvement of both the position and time resolution attainable in experiments. To provide some insight into the improvement in tracking made solely on the basis of improvement in camera technology, let us compare the specifications of a modern scientific CMOS camera (Neo sCMOS, Andor) with the specifications of the camera used by Strick et al. in their early demonstration of single-molecule magnetic tweezers 15 years ago (XC-77CE, Sony) (83, 85). We consider an effective field of view size of $10^4 \mu\text{m}^2$ for both camera systems. The modern camera has 5.5×10^6 pixels, whereas the old camera has only 0.4×10^6 pixels; an image of the same sized area in the flow cell thus comprises 14 times more pixels on the modern camera. Furthermore, modern cameras offer much higher frame rates than the camera originally used by Strick et al., in particular when use is made of an adjustable region of interest. We assume a frame rate of 1 kHz, a conservative number given several recent demonstrations of real-time position tracking at frequencies up to 15,000 frames per second (9, 75, 76, 91, 96) but much higher than the frame rate obtained with the old camera (25 Hz). Following Equation 3, we find that the position resolution is improved with a factor of 24 solely on the basis of the better camera technology available today.¹ Thermal-force-limited performance of magnetic tweezers is thus in principle achievable even for high forces (>10 pN) applied to short molecules ($<1 \mu\text{m}$).

Second, other means to enhance tracking resolution can furthermore be found in nondiffraction-based measurements of the bead height. Kim & Saleh (43, 44) achieved enhanced resolution and subnanometer accuracy in measurements of bead height by exploiting reflection interference contrast microscopy. Another option is found in an alternative configuration of magnetic tweezers in which the DNA is pulled sideways (35, 54). In this side-pulling mode, the tether length is determined on the basis of measurements of the lateral position of the bead, thus along the axis for which fast, high-precision video-microscopy-based position measurements can be performed. High-resolution measurements based on side-pulling magnetic tweezers have not been pursued thus far.

Last, when studying reactions accompanied by a change in DNA topology, use can be made of the coupling between topology and length in plectonemic DNA (78, 79, 93). The removal or addition of supercoils to DNA leads to a strong, force-dependent change in length, on the

¹At high frame rates and low magnification, illumination may become limiting. Powerful LEDs, incandescent lamps, or laser illumination, however, can be considered in an attempt to increase the number of photons detected per frame and per pixel.

order of 50 nm per coil, or 5 nm per base. Accordingly, enzymes that change DNA topology can give rise to tether-length changes even greater than the footprint of the enzyme on the DNA. Revyakin et al. (78) were the first to exploit this principle and to apply it to the measurement of the RNA-polymerase-driven unwinding of a single turn of promoter DNA.

These recent developments indicate that limitations in camera-based tracking can be alleviated, making magnetic tweezers a versatile platform for high-resolution single-molecule experiments. The inherent insensitivity of magnetic tweezers to sources of low-frequency noise significantly reduces the cost and complexity of setup design and allows facile and long-term high-resolution operation with minimal instrument start-up time. Of further interest, high-resolution magnetic tweezers measurements can in principle be performed on many molecules in parallel. Recent efforts in parallelism are the subject of the next section.

FROM SINGLE-MOLECULE TO KILO-MOLECULE MAGNETIC TWEEZERS

Single-molecule-manipulation methods generally suffer from low experimental throughput, as typically only one molecule is addressed in an individual experiment. Limitations in experimental throughput make it cumbersome to extract ensemble-level information and to investigate possible rare events in DNA-protein interactions. Both the magnetic-force-based manipulation and the camera-based detection used in magnetic tweezers are compatible with multiplexed measurements. Magnetic tweezers thus naturally lend themselves to parallel measurements, in contrast to other single-molecule manipulation techniques such as optical tweezers and atomic force microscopy. See **Figure 3a** for a schematic of multiplexing in magnetic tweezers. Parallelism has been exploited in magnetic-tweezers-based lifetime measurements of annealed/ligated DNA assemblies (7) and ligand-receptor complex bonds (24). Recently, Ribeck & Saleh (80) provided the first demonstration of controlled parallel single-DNA manipulation with magnetic tweezers. Multiplexed magnetic tweezers have since been used in high-throughput studies of the DNA cleavage activity of type III restriction enzymes (39, 77), the effect of force on collagen

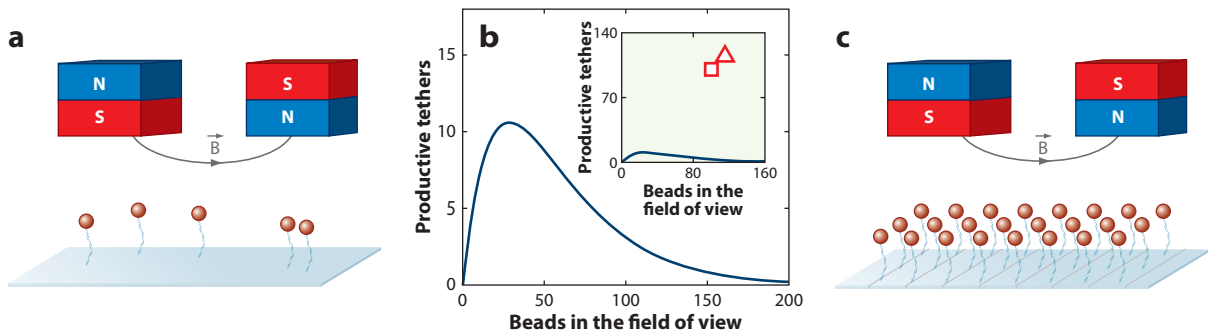


Figure 3

Highly parallel single-molecule magnetic tweezers. (a) Both the magnetic-force-based manipulation and the camera-based detection used in magnetic tweezers are compatible with multiplexed measurements. (b) A random distribution of DNA-bead tethers leads to poor occupation of the field of view space. A maximum of 10 productive DNA-bead tethers can be found in a $100 \times 100 \mu\text{m}$ field of view (criterion chosen here: nearest neighbor spacing $> 10 \mu\text{m}$). The inset compares the expected number of productive tethers for a random square array (square) and hexagonal array (triangle). (c) Directed surface tethering in regular arrays yields an improvement of one order of magnitude in density of productive tethers on the surface (26). Abbreviations: N, magnetic north pole; S, magnetic south pole.

proteolysis by matrix metalloproteinase-1 (3), and the effect of the C-terminal RAD51 interaction domain of the breast cancer tumor suppressor BRCA2 on the formation of Rad51 filaments on DNA (92).

What are the ultimate limits of multiplexing in magnetic tweezing? What kind of measures must be taken in order to push the level of parallelism in magnetic tweezers toward the simultaneous measurement of 1,000 molecules (26, 80)?

Microcontact printing: soft lithography technique used to create a patterned protein layer on a substrate

See More Beads

First and foremost, parallel magnetic-tweezers-based measurements of many molecules require that the camera images many DNA-bead tethers. This can be achieved most easily by expanding the size of the imaging field of view, which in turn can be realized through the use of a larger camera array and/or through a reduction of the magnification of the imaging system. A lower magnification of the imaging system unavoidably leads to a lower resolution in tracking (80); thus, using a larger camera, if possible, is preferred.

Another factor that limits the number of beads is the density of DNA-bead tethers on the surface of the flow cell. The standard surface-tethering protocols used in magnetic tweezers (99) give rise to a random distribution of DNA-bead tethers on the surface. **Figure 3b** shows the theoretical number of productive DNA-bead tethers that can be found in a $100 \times 100 \mu\text{m}$ field of view as a function of the total number of beads in this field of view, following equation 2 in Reference 26. Here, we define a DNA-bead tether as potentially productive in experiments when spaced farther than $10 \mu\text{m}$ away from its nearest neighbor and at least $5 \mu\text{m}$ away from the border of the field of view. Optimizing the concentration of the bead-DNA tethers on the surface leads to a maximum of 10 productive DNA-bead tethers. This is a relatively low number if one considers that 100 (115) DNA-bead tethers organized in a regular square (hexagonal) array fit the same $100 \times 100 \mu\text{m}$ field of view. Regular arrays of DNA-bead tethers thus lead to an increase of more than one order of magnitude in throughput in magnetic tweezers experiments (**Figure 3c**). In Reference 26, targeted binding of DNA-bead tethers to form such regular arrays was achieved via microcontact printing of DNA-end-binding labels on the surface of the flow cell. This method allowed as many as 356 DNA-bead tethers found in a $300 \times 400 \mu\text{m}$ field of view to be mechanically measured in parallel (26).

After solving the problem of capturing many beads in the camera field of view, one encounters the difficulty of tracking simultaneously the xyz positions of all the beads during the experiment. Ribeck & Saleh (80) achieved real-time tracking of up to 34 beads at a 60 Hz frame rate, and fast, video-microscopy-based position tracking has been achieved in optical tweezers experiments and has allowed for high-frequency measurements (up to 6,000 fps) of the position fluctuations of a bead trapped in a high-stiffness optical trap (76). Real-time tracking becomes cumbersome when tracking a significantly higher number of beads ($>1,000$) is desired. In this case a scalable alternative is the offline analysis of images recorded and saved during the experiment (26).

Stretch More Molecules

In contrast to single-molecule manipulation techniques based on optical trapping or cantilever actuation, the magnet-based manipulation employed in magnetic tweezers is well suited for parallel manipulation of many molecules simultaneously, as forces can be applied to many beads distributed over a wide, millimeter-scale flow cell area. All beads do not necessarily experience the same force, however (7). The force can vary substantially across the field of view area, particularly when a large field of view system is used. Variations of the force field depend on the specific magnet

configuration and the position of the magnet with respect to the beads. Field variations should be corrected for, for example, by following predictions from three-dimensional modeling, or alternatively, after experimental characterization of the angle of the force. The latter can be achieved by analyzing the rotational pattern of a DNA-bead tether subject to a rotating magnetic field, which describes a bicircular pattern that is an example of a Limaçon roulette (I. De Vlaminck, T. Henighan, M. van Loenhout, D. Burnham & C. Dekker, manuscript submitted).

More Is More

These recent developments pave the way to routine, highly parallelized magnetic tweezers experiments (50). Multiplexed magnetic tweezers will benefit from ongoing developments in camera technology that will make faster and larger cameras with smaller pixels available to experimentalists. We therefore anticipate that kilo-molecule-level magnetic tweezers measurements will be readily possible in the near future. Kilo-molecule-level experiments allow single experimental run measurements of the statistical distribution of reaction times, reducing the total experiment time and removing variability in buffer conditions and enzyme concentration. Multiplexed magnetic tweezers thereby greatly facilitate performing force spectroscopy or torque spectroscopy analyses of DNA-enzyme interactions.² Highly multiplexed magnetic tweezers provide direct information about ensemble behavior while remaining sensitive to sample heterogeneity. Multiplexed magnetic tweezers thus also provide a means to rigorously study infrequent events in DNA-protein interactions.

MEASUREMENTS OF TORQUE

A hallmark of magnetic tweezers is its ability to apply torque to a tethered molecule. By simply rotating the external magnetic field and thereby rotating the magnetic bead, the molecule can be mechanically coiled provided that the molecule is rotationally constrained, meaning that it does not carry any nicks (i.e., breaks in one of the strands) and that both strands are attached at both ends of the molecule. The supercoil density, defined as $\sigma = (Lk - Lk_0)/Lk_0$, where Lk_0 and Lk are the linking numbers of the relaxed and supercoiled DNA, respectively (88), can be changed accordingly. The change in linking number is stored in the molecule as a change in twist or writhe, where twist refers to the number of twists or turns within the molecule and writhe to the number of plectonemes. The torque stored in an overwound or underwound molecule ($\sigma > 0$ or $\sigma < 0$, respectively) is a function of the applied force and the supercoil density.

Various closed-form analytical expressions describe the torque in twisted and plectonemic DNA (65, 68, 84, 88). Direct measurements of torque or direct measurements of changes in the linking number of the tethered molecule are not, however, readily possible with magnetic tweezers. Such measurements are precluded by the strong torque generated by the asymmetric magnetic field in the standard magnetic tweezers configuration that rotationally clamps the bead (see schematic in **Figure 4a**). The torque experienced by the paramagnetic bead in the magnetic field ($\sim 10^4$ – 10^5 pN nm rad^{−1}) dominates the typical torque stored in the molecule (on the order of 10 pN nm), and direct measurements of torque therefore require a high resolution in measurements of the equilibrium angle of the bead, $\delta\theta < 10^{-3}$ – 10^{-4} . It is possible to measure torque in DNA indirectly

²The above-described variations in force applied to tethers across the field of view can be utilized to extract the force dependence of reaction rates, again from data obtained in a single experimental run. As an alternative, one can think of experiments with different sized magnetic beads to apply different forces on different molecules.

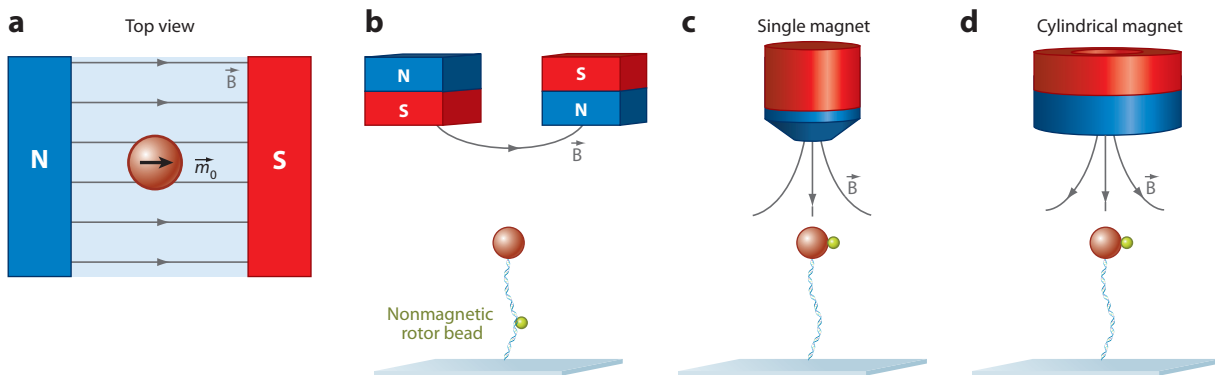


Figure 4

Torque-sensitive magnetic tweezers. (a) Top view of the conventional implementation of magnetic tweezers. Here, a strong asymmetric magnetic field acts as a torque clamp on the bead and precludes direct probing of the torque stored in the DNA tether. Torque-and-twist-sensitive magnetic tweezers (6, 16, 33, 38, 60, 61, 69) rely on a reduction of the torque exerted by the magnets to allow for (near-) free rotation of the magnetic bead or a nonmagnetic rotor bead attached to the molecular tether (as shown in the side view in panel b). (c,d) Side views of configurations that rely on circularly symmetric fields generated by (c) a single magnet or (d) a cylindrical magnet. Abbreviations: N, magnetic north pole; S, magnetic south pole.

by using magnetic tweezers. Strick et al. (87) determined torque from measurements of the extra work required to stretch a molecule when underwound or overwound. A related method relies on integrating the change in extension per change in linking number (104). Mosconi et al. (69) used the latter approach to probe the torsional modulus of DNA in a wide force range. However, these indirect methods are restricted to static measurements on plectonemic DNA.

The lack of methodology for the direct measurement of twist and torque in magnetic tweezers represented a hiatus that was removed by a number of recent reports of torque-and-twist-sensitive magnetic tweezers. The common theme in these schemes is a reduction of the magnetic background torque to levels similar to or smaller than the torque stored in the molecular tether. Gore et al. (33) made use of a nonmagnetic rotor bead attached along the length of the molecule to sensitively measure twist (Figure 4b). With this assay they investigated how twist in the DNA helix changes upon stretching. Remarkably, they found that DNA overwinds when stretched with applied forces as high as ~ 30 pN, and that DNA thus has a negative twist-stretch coupling in this force range ($g = -90 \pm 20$ pN nm) (57). In another recent contribution Celedon et al. (16) describe magnetic tweezers with a cylindrical magnet configuration that produces a magnetic field that is circularly symmetric about the central axis of the magnet (Figure 4d). A DNA-bead tether aligned to the center of this magnet experiences a soft torque clamp. Celedon et al. use a magnetic nanowire bead assembly as probe and measure torque from the horizontal angular fluctuations of this probe. The torque clamp in this scheme was sufficiently strong to coil the DNA, and these authors were able to measure the torque in plectonemic DNA as a function of force. A good agreement was found between results obtained with optical torque tweezers (30) and a theory by Marko (65). These authors furthermore showed that the torsional rigidity of chromatin fibers is lower than the torsional rigidity of bare DNA. In another contribution, Lipfert et al. (60) used a weak torque clamp magnet configuration consisting of a cylindrical magnet with circularly symmetric magnetic field in conjunction with a small side magnet that superimposes a weak asymmetric field. A small marker bead attached to the magnetic bead allows high-precision tracking ($\delta\theta \approx 0.1^\circ$) of angular fluctuations of the bead (59). Lipfert et al. measured

the torsional stiffness of bare DNA as a function of coiling number over a wide force range ($F = 0.25\text{--}6.5\text{ pN}$) and performed measurements of the torsional compliance of a RecA nucleoprotein filament.

Instruments with a magnet configuration that generates a magnetic field with near-zero torque in which the magnetic bead is free to rotate or orbit enable real-time tracking of changes in twist in DNA. A single magnet aligned to the DNA-bead tether (Figure 4c) generates such zero-torque field and was used by Harada et al. (38) to study DNA rotation during transcription of *Escherichia coli* RNA polymerase. The same configuration was used in measuring polymerization of Rad51 on DNA (6). Lipfert et al. (61) used a carefully aligned cylindrical magnet and tracked polymerization of RecA on dsDNA. Last, Mosconi et al. (70) achieved a soft magnetic torque trap based on the observation that a magnetic bead can only follow the rotations of a spinning magnetic field up to a magnetic-field-strength-dependent and bead-size-dependent breakdown frequency (41). An arbitrarily small torque can in principle be achieved with a fast-spinning externally applied magnetic field (70).

These newly developed torque-and-twist-sensitive magnetic tweezers provide a new mode with which to probe DNA-enzyme interactions and provide access to structural information that is hard to obtain. It remains to be seen how this new platform can be applied to measurements of dynamics. The time resolution attainable in mechanical measurements of DNA is set by the drag on the bead, γ , and the stiffness of the molecule, k . The characteristic response time of the mechanical system can be calculated from $\tau_c = \gamma/k$. The torsional compliance of DNA is relatively weak compared to its stretch stiffness, and the time resolution of the above-described methods is thus intrinsically low compared to length-based measurements. As an example, twist measurements on a molecule with length $l_c = 2.6\text{ }\mu\text{m}$ and bead radius $R_{bead} = 1.5\text{ }\mu\text{m}$ yield $\tau_c \sim 1,000\text{ s}$ (61), whereas length measurements on the same system yield $\tau_c = 0.9\text{ ms}$ at an applied force $F = 10\text{ pN}$, i.e., six orders of magnitude faster. Improvements in time resolution can be obtained for shorter molecules and smaller rotary probes. For those schemes where the magnetic bead serves the dual purpose of rotary tracking and force transduction, downscaling the probe strongly reduces the maximum applicable force ($F_{max} \sim R_{bead}^3$). The approach taken by Gore et al. (33), in which a nonmagnetic rotary probe is used in conjunction with a magnetic bead for force transduction, is particularly appealing because it allows independent optimization of F_{max} and τ_c .

HYBRID INSTRUMENTS

Next, we describe recent developments of hybrid instruments in which magnetic tweezers are combined with alternative single-molecule manipulation techniques and/or fluorescence detection methods. These hybrid instruments further extend the arsenal of measurement capabilities of magnetic tweezers to the direct measurements of (protein-mediated) DNA-DNA interactions, (co)localization of DNA-bound proteins, and measurements of intrinsically weak DNA-enzyme interactions.

Magnetic Tweezers Meet Optical Tweezers

In a sense, the term magnetic tweezers is misleading: The magnetic field generated by the magnets does not produce an energy potential landscape in which the motion of the magnetic bead is restricted in three dimensions, and with the notable exception of specialized implementations using feedback-operated electromagnets (34), it is not possible to hold and controllably manipulate magnetic particles in three dimensions using magnetic tweezers. Three-dimensional manipulation

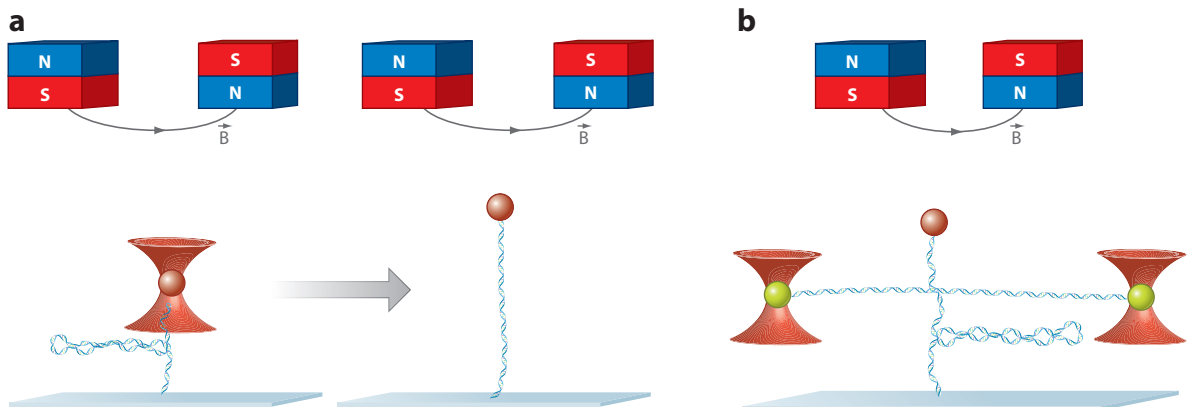


Figure 5

Magnetic tweezers integrated with optical tweezers. (a) A single-beam optical trap reduces the end-to-end distance of a molecule. The tethers experience a near-instantaneous change in force upon switching off (arrow) the laser trap. Crut et al. (22) used such a configuration to study the dynamic relaxation of DNA plectonemes. (b) Dual-bead optical tweezers integrated with magnetic tweezers for the independent manipulation of two DNA molecules and for probing their mutual (protein-mediated) interactions. Abbreviations: N, magnetic north pole; S, magnetic south pole.

capabilities are a hallmark of optical tweezers (67), and optical tweezers instrumentation has been developed for trapping many beads (>100) simultaneously (71). Dame et al. (23) manipulated two distinct molecules of DNA attached to four optically trapped beads and they used this configuration to probe DNA-DNA interactions mediated by the histone-like nucleoid structuring protein. Magnetic-tweezers-only measurements of intermolecular reactions (8) have relied on a configuration in which the magnetic bead is tethered by two or more molecules. Such a configuration can be isolated after careful mechanical characterization (17).

The co-integration of magnetic tweezers with optical tweezers is particularly interesting for dual-molecule interaction studies and combines the advantages of both techniques. Crut et al. (22) described the first demonstration of an instrument in which optical and magnetic tweezers were combined. The authors combined an optical trap with magnetic tweezers to allow for near-instantaneous changes in applied force in an attempt to probe the dynamics of plectoneme release (see Figure 5a) (22). We have recently combined magnetic tweezers with dual-bead optical tweezers with the purpose of dual-molecule interaction experiments (I. De Vlaminck, M. van Loenhout, L. Zweifel, J. den Blanken, K. Hooning, et al., manuscript submitted). Figure 5b shows a schematic of the assay developed. The dual-bead optical tweezers provide nanometer-scale precision of positioning a molecular substrate in proximity to the molecular tether held in magnetic tweezers. The magnetic tweezers can be used as a sensitive force probe with ideal force-clamp characteristics. Forces are inferred from lateral movements of the magnetic bead, along the direction for which video-microscopy-based position measurements can be performed with high precision. The force resolution in this configuration is set by the Langevin force noise acting on the bead ($F_n = \sqrt{12\pi k_B T \eta R dt}$). The molecular substrate in the magnetic tweezers configuration can be supercoiled, and the effects of twist and torque on intermolecular interactions can thus be explored.

We anticipate that such hybrid systems in which multiple molecules can be manipulated and interacted will be applicable to the study of a wide range of complex systems. Potential experiments and subjects of study include higher-order chromatin interactions; DNA-DNA interactions mediated by proteins, e.g., bridging proteins and reactions involved in homologous recombination;

measurements of intermolecular friction; and localization and binding strength analyses of DNA-bound proteins (74).

Combinations with Fluorescence Microscopy

In all modes of operation of magnetic tweezers considered so far, information on the dynamics of enzyme on DNA is inferred from measurements of the length or the linking number of the molecular tether. Such measurements come with a number of intrinsic limitations. Information on the location of enzymatic activity along the length of the molecule is lost. Moreover, these measurement modes are applicable exclusively to relatively strong DNA-enzyme interactions that give rise to measurable changes in length or linking number, and cannot readily be employed in the study of weak interactions, e.g., the interactions arising during the diffusive sliding of enzymes along DNA (10).

Fluorescence microscopy techniques (42), on the other hand, enable investigators to study (sub)millisecond dynamics of weak DNA-enzyme interactions, where information on the location of the reaction is retained. Furthermore, fluorescence microscopy techniques provide direct interpretation of data with little ambiguity (100). Fluorescence microscopy techniques, however, cannot be used to controllably change the conformation of the molecule or to investigate the influence of torque and force on reaction dynamics.

The combination of fluorescence microscopy and single-molecule manipulation (15, 98) brings together the best of both worlds. The combination of fluorescence microscopy and magnetic tweezers in a hybrid instrument is particularly powerful given the simplicity of implementation of magnetic tweezers, the accessibility of DNA supercoiling, and the absence of a strong light source required for DNA manipulation that may interfere with fluorescence detection (42).

In the standard implementation of magnetic tweezers, the DNA is stretched in the direction perpendicular to the image plane, and therefore only a short segment of the molecule can be brought into focus. If the optical probes are located close to the flow cell surface, total internal reflection fluorescence microscopy can be used (40, 62) (see **Figure 6a**). Schroff et al. (81) reported on Förster resonance energy transfer (FRET) (89) measurements of the distance between two fluorophores attached to a single-stranded DNA as a function of the force applied to the molecule with magnetic tweezers. Hugel et al. (40) probed the rotational motion of a fluorescent probe attached to a rotary motor using polarization-sensitive fluorescent microscopy. In another example of a combination of magnetic tweezers and FRET microscopy, Lee et al. (53) exploited the possibility to supercoil DNA substrates and applied it to the study of the energetics of left-handed Z-DNA and B-DNA to Z-DNA transitions. When the magnet configuration is adapted to allow stretching of the molecule in the imaging plane (see **Figure 6b**), the entire molecule can be visualized (35, 36). Graham et al. (36) used such a configuration to visualize and count proteins bound to a single DNA molecule.

The sensitivity and time resolution accessible with fluorescence techniques combined with the possibility to supercoil DNA with magnetic tweezers allow investigators to explore important yet experimentally uncharted terrain in DNA mechanics: the dynamics of diffusion and hopping of plectonemes in DNA and the influence of twist and torque on intrinsic DNA-breathing dynamics.

CONCLUSIONS AND OUTLOOK

Given their ease of use and simplicity of implementation, combined with their single-molecule sensitivity and the capability to supercoil DNA, magnetic tweezers hold the promise of becoming a ubiquitous tool in molecular biology. To fulfill this promise, large-scale parallelism with routine,

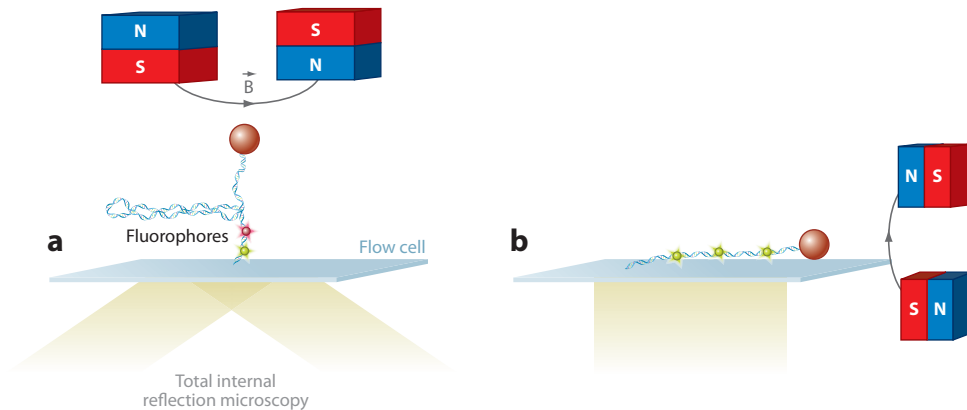


Figure 6

A combination of magnetic tweezers and fluorescence microscopy. (a) Dynamic and sensitive measurements of the length or topology of a DNA segment taken from measurements of Förster resonance energy transfer (FRET) between two fluorophores located near the surface of the flow cell (53, 81). Total internal reflection illumination reduces the background from free proteins. (b) Stretching of the molecule in the imaging plane can be used to visualize proteins bound along the length of the DNA (36) or to probe weak DNA-protein interactions. Abbreviations: N, magnetic north pole; S, magnetic south pole.

simultaneous measurements on many molecules (100–1,000) and high-resolution magnetic tweezers with resolution on par with state-of-the art optical tweezers need to be established. Recent developments of torque-and-twist-sensitive magnetic tweezers and demonstrations of magnetic tweezers integrated into alternative single-molecule manipulation and optical spectroscopy techniques allow an ever larger parameter space to be accessed. There is no doubt that 20 years after their introduction, magnetic tweezers will continue to attract a lot of attention.

SUMMARY POINTS

1. Single-molecule magnetic tweezers have been applied in the study of a broad range of biophysical systems.
2. Recent technical improvements expand the parameter space accessible with magnetic tweezers.
3. New methods and improved computer and camera hardware make highly parallel magnetic tweezers possible.
4. Camera-technology-driven improvements in video-based microscopy enable high-resolution position measurements in magnetic tweezers.
5. Torque-and-twist-sensitive magnetic tweezers have been developed.
6. Combinations with fluorescence microscopy and optical tweezers have been demonstrated.

DISCLOSURE STATEMENT

The authors are not aware of any affiliations, memberships, funding, or financial holdings that might be perceived as affecting the objectivity of this review.

ACKNOWLEDGMENTS

We thank the members of the Cees Dekker lab and the Nynke Dekker lab for stimulating discussions. We are grateful to Marijn van Loenhout, David Dulin, Jan Lipfert, and Daniel Burnham for critical reading of the manuscript. This work was supported by a DNA-in-action grant from the Stichting voor Fundamenteel Onderzoek der Materie (FOM), which is financially supported by the Nederlandse Organisatie voor Wetenschappelijk Onderzoek (NWO) and a European Research Council (ERC) grant.

LITERATURE CITED

1. Abbondanzieri EA, Greenleaf WJ, Shaevitz JW, Landick R, Block SM. 2005. Direct observation of base-pair stepping by RNA polymerase. *Nature* 438:460–65
2. Abels JA, Moreno-Herrero F, van der Heijden T, Dekker C, Dekker NH. 2005. Single-molecule measurements of the persistence length of double-stranded RNA. *Biophys. J.* 88:2737–44
3. Adhikari AS, Chai J, Dunn AR. 2011. Mechanical load induces a 100-fold increase in the rate of collagen proteolysis by MMP-1. *J. Am. Chem. Soc.* 133:1686–89
4. Allemand J-F, Bensimon D, Croquette V. 2003. Stretching DNA and RNA to probe their interactions with proteins. *Curr. Opin. Struct. Biol.* 13:266–74
5. Allemand JF, Bensimon D, Lavery R, Croquette V. 1998. Stretched and overwound DNA forms a Pauling-like structure with exposed bases. *Proc. Natl. Acad. Sci. USA* 95:14152–57
6. Arata H, Dupont A, Miné-Hattab J, Disseau L, Renodon-Cornière A, et al. 2009. Direct observation of twisting steps during Rad51 polymerization on DNA. *Proc. Natl. Acad. Sci. USA* 106:19239–44
7. Assi F, Jenks R, Yang J, Love C, Prentiss M. 2002. Massively parallel adhesion and reactivity measurements using simple and inexpensive magnetic tweezers. *J. Appl. Phys.* 92:5584
8. Bai H, Sun M, Ghosh P, Hatfull GF, Grindley ND, Marko JF. 2011. Single-molecule analysis reveals the molecular bearing mechanism of DNA strand exchange by a serine recombinase. *Proc. Natl. Acad. Sci. USA* 108:7419–24
9. Biancaniello PL, Crocker JC. 2006. Line optical tweezers instrument for measuring nanoscale interactions and kinetics. *Rev. Sci. Instrum.* 77:113702
10. Blainey PC, van Oijen AM, Banerjee A, Verdine GL, Xie XS. 2006. A base-excision DNA-repair protein finds intrahelical lesion bases by fast sliding in contact with DNA. *Proc. Natl. Acad. Sci. USA* 103:5752–57
11. Bouchiat C, Wang MD, Allemand JF, Strick T, Block SM, Croquette V. 1999. Estimating the persistence length of a worm-like chain molecule from force-extension measurements. *Biophys. J.* 76:409–13
12. Brown LG. 1992. A survey of image registration techniques. *ACM Comput. Surv.* 24:325–76
13. Bustamante C, Bryant Z, Smith SB. 2003. Ten years of tension: single-molecule DNA mechanics. *Nature* 421:423–27
14. Bustamante C, Smith SB, Liphardt J, Smith D. 2000. Single-molecule studies of DNA mechanics. *Curr. Opin. Struct. Biol.* 10:279–85
15. Candelli A, Wuite GJL, Peterman EJG. 2010. Combining optical trapping, fluorescence microscopy and micro-fluidics for single molecule studies of DNA-protein interactions. *Phys. Chem. Chem. Phys.* 13:7263–72
16. Celedon A, Nodelman IM, Wildt B, Dewan R, Searson P, et al. 2009. Magnetic tweezers measurement of single molecule torque. *Nano Lett.* 9:1720–25
17. Charvin G, Vologodskii A, Bensimon D, Croquette V. 2005. Braiding DNA: experiments, simulations, and models. *Biophys. J.* 88:4124–36

18. Cheezum MK, Walker WF, Guilford WH. 2001. Quantitative comparison of algorithms for tracking single fluorescent particles. *Biophys. J.* 81:2378–88

19. Cheng W, Arunajadai SG, Moffitt JR, Tinoco I, Bustamante C. 2011. Single base pair unwinding and asynchronous RNA release by the hepatitis C virus NS3 helicase. *Science* 333:1746–49

20. Crick F. 1950. The physical properties of cytoplasm: a study by means of the magnetic particle method. Part II. Theoretical treatment. *Exp. Cell Res.* 1:505–33

21. Crick FHC, Hughes AFW. 1950. The physical properties of cytoplasm: a study by means of the magnetic particle method. Part I. Experimental. *Exp. Cell Res.* 1:37–80

22. Crut Al, Koster DA, Seidel R, Wiggins CH, Dekker NH. 2007. Fast dynamics of supercoiled DNA revealed by single-molecule experiments. *Proc. Natl. Acad. Sci. USA* 104:11957–62

23. Dame RT, Noom MC, Wuite GJL. 2006. Bacterial chromatin organization by H-NS protein unravelled using dual DNA manipulation. *Nature* 444:387–90

24. Danilowicz C, Greenfield D, Prentiss M. 2005. Dissociation of ligand-receptor complexes using magnetic tweezers. *Anal. Chem.* 77:3023–28

25. Dawid A, Croquette V, Grigoriev M, Heslot F. 2004. Single-molecule study of RuvAB-mediated Holliday-junction migration. *Proc. Natl. Acad. Sci. USA* 101:11611–16

26. De Vlaminck I, Henighan T, van Loenhout MT, Pfeiffer I, Huijts J, et al. 2011. Highly parallel magnetic tweezers by targeted DNA tethering. *Nano Lett.* 11:5489–93

27. De Vlaminck I, Vidic I, van Loenhout MTJ, Kanaar R, Lebbink JHG, Dekker C. 2010. Torsional regulation of hRPA-induced unwinding of double-stranded DNA. *Nucleic Acids Res.* 38:4133–42

28. Dessinges MN, Lionnet T, Xi XG, Bensimon D, Croquette V. 2004. Single-molecule assay reveals strand switching and enhanced processivity of UvrD. *Proc. Natl. Acad. Sci. USA* 101:6439–44

29. Fisher J, Cribb J, Desai K, Vicci L, Wilde B, et al. 2006. Thin-foil magnetic force system for high-numerical-aperture microscopy. *Rev. Sci. Instrum.* 77:023702

30. Forth S, Deufel C, Sheinin MY, Daniels B, Sethna JP, Wang MD. 2008. Abrupt buckling transition observed during the plectoneme formation of individual DNA molecules. *Phys. Rev. Lett.* 100:148301

31. Gelles J, Schnapp BJ, Sheetz MP. 1988. Tracking kinesin-driven movements with nanometre-scale precision. *Nature* 331:450–53

32. Gittes F, Schmidt CF. 1998. Thermal noise limitations on micromechanical experiments. *Eur. Biophys. J.* 27:75–81

33. Gore J, Bryant Z, Nöllmann M, Le MU, Cozzarelli NR, Bustamante C. 2006. DNA overwinds when stretched. *Nature* 442:836–39

34. Gosse C, Croquette V. 2002. Magnetic tweezers: micromanipulation and force measurement at the molecular level. *Biophys. J.* 82:3314–29

35. Graham JS, Johnson RC, Marko JF. 2011. Concentration-dependent exchange accelerates turnover of proteins bound to double-stranded DNA. *Nucleic Acids Res.* 39:2249–59

36. Graham JS, Johnson RC, Marko JF. 2011. Counting proteins bound to a single DNA molecule. *Biochem. Biophys. Res. Commun.* 415:131–34

37. Haber C, Wirtz D. 2000. Magnetic tweezers for DNA micromanipulation. *Rev. Sci. Instrum.* 71:4561–70

38. Harada Y, Ohara O, Takatsuki A, Itoh H, Shimamoto N, Kinosita K. 2001. Direct observation of DNA rotation during transcription by *Escherichia coli* RNA polymerase. *Nature* 409:113–15

39. Holthausen JT, van Loenhout MTJ, Sanchez H, Ristic D, van Rossum-Fikkert SE, et al. 2011. Effect of the BRCA2 CTRD domain on RAD51 filaments analyzed by an ensemble of single molecule techniques. *Nucleic Acids Res.* 39:6558–67

40. Hugel T, Michaelis J, Hetherington CL, Jardine PJ, Grimes S, et al. 2007. Experimental test of connector rotation during DNA packaging into bacteriophage ϕ 29 capsids. *PLoS Biol.* 5:e59

41. Janssen XJA, Schellekens AJ, van Ommering K, van IJzendoorn LJ, Prins MWJ. 2009. Controlled torque on superparamagnetic beads for functional biosensors. *Biosens. Bioelectron.* 24:1937–41

42. Joo C, Balci H, Ishitsuka Y, Buranachai C, Ha T. 2008. Advances in single-molecule fluorescence methods for molecular biology. *Annu. Rev. Biochem.* 77:51–76

43. Kim K, Saleh OA. 2008. Stabilizing method for reflection interference contrast microscopy. *Appl. Opt.* 47:2070–75

21. First demonstration of magnetic actuation of motion.

33. Twist-sensitive-magnetic tweezers and measurement of twist-stretch coupling.

44. Kim K, Saleh OA. 2009. A high-resolution magnetic tweezer for single-molecule measurements. *Nucleic Acids Res.* 37:e136
45. Klaue D, Seidel R. 2009. Torsional stiffness of single superparamagnetic microspheres in an external magnetic field. *Phys. Rev. Lett.* 102:028302
46. Kollmannsberger P, Fabry B. 2007. High-force magnetic tweezers with force feedback for biological applications. *Rev. Sci. Instrum.* 78:114301–6
47. Koster DA, Croquette V, Dekker C, Shuman S, Dekker NH. 2005. Friction and torque govern the relaxation of DNA supercoils by eukaryotic topoisomerase IB. *Nature* 434:671–74
48. Koster DA, Crut A, Shuman S, Bjornsti M-A, Dekker NH. 2010. Cellular strategies for regulating DNA supercoiling: a single-molecule perspective. *Cell* 142:519–30
49. Koster DA, Palle K, Bot ESM, Bjornsti M-A, Dekker NH. 2007. Antitumour drugs impede DNA uncoiling by topoisomerase I. *Nature* 448:213–17
50. Kruithof M, Chien F, de Jager M, van Noort J. 2008. Subpiconewton dynamic force spectroscopy using magnetic tweezers. *Biophys. J.* 94:2343–48
51. Kruithof M, Chien F-T, Routh A, Logie C, Rhodes D, van Noort J. 2009. Single-molecule force spectroscopy reveals a highly compliant helical folding for the 30-nm chromatin fiber. *Nat. Struct. Mol. Biol.* 16:534–40
52. Lavelle C. 2008. DNA torsional stress propagates through chromatin fiber and participates in transcriptional regulation. *Nat. Struct. Mol. Biol.* 15:123–25
53. Lee M, Kim SH, Hong S-C. 2010. Minute negative superhelicity is sufficient to induce the B-Z transition in the presence of low tension. *Proc. Natl. Acad. Sci. USA* 107:4985–90
54. Leuba SH, Karymov MA, Tomschik M, Ramjit R, Smith P, Zlatanova J. 2003. Assembly of single chromatin fibers depends on the tension in the DNA molecule: magnetic tweezers study. *Proc. Natl. Acad. Sci. USA* 100:495–500
55. Lionnet T, Allemand JF, Revyakin A, Strick TR, Saleh OA, et al. 2008. Single-molecule studies using magnetic traps. *Single Mol. Tech. Lab. Manual* 347:34–39
56. Lionnet T, Dawid A, Bigot S, Barre F-X, Saleh OA, et al. 2006. DNA mechanics as a tool to probe helicase and translocase activity. *Nucleic Acids Res.* 34:4232–44
57. Lionnet T, Joubaud S, Lavery R, Bensimon D, Croquette V. 2006. Wringing out DNA. *Phys. Rev. Lett.* 96:178102
58. Lipfert J, Hao X, Dekker NH. 2009. Quantitative modeling and optimization of magnetic tweezers. *Biophys. J.* 96:5040–49
59. Lipfert J, Kerssemakers JJ, Rojer M, Dekker NH. 2011. A method to track rotational motion for use in single-molecule biophysics. *Rev. Sci. Instrum.* 82:103707
60. Lipfert J, Kerssemakers JW, Jager T, Dekker NH. 2010. Magnetic torque tweezers: measuring torsional stiffness in DNA and RecA-DNA filaments. *Nat. Methods* 7:977–80
61. Lipfert J, Wiggin M, Kerssemakers JW, Pedaci F, Dekker NH. 2011. Freely orbiting magnetic tweezers to directly monitor changes in the twist of nucleic acids. *Nat. Commun.* 2:439
62. Liu R, Garcia-Manyes S, Sarkar A, Badilla CL, Fernández JM. 2009. Mechanical characterization of protein L in the low-force regime by electromagnetic tweezers/evanescent nanometry. *Biophys. J.* 96:3810–21
63. Maier B, Bensimon D, Croquette V. 2000. Replication by a single DNA polymerase of a stretched single-stranded DNA. *Proc. Natl. Acad. Sci. USA* 97:12002–7
64. Manosas M, Xi XG, Bensimon D, Croquette V. 2010. Active and passive mechanisms of helicases. *Nucleic Acids Res.* 38:5518–26
65. Marko JF. 2007. Torque and dynamics of linking number relaxation in stretched supercoiled DNA. *Phys. Rev. E* 76:021926
66. Moffitt JR, Chemla YR, Izhaky D, Bustamante C. 2006. Differential detection of dual traps improves the spatial resolution of optical tweezers. *Proc. Natl. Acad. Sci. USA* 103:9006–11
67. Moffitt JR, Chemla YR, Smith SB, Bustamante C. 2008. Recent advances in optical tweezers. *Annu. Rev. Biochem.* 77:205–28
68. Moroz JD, Nelson P. 1997. Torsional directed walks, entropic elasticity, and DNA twist stiffness. *Proc. Natl. Acad. Sci. USA* 94:14418–22

69. Mosconi F, Allemand JF, Bensimon D, Croquette V. 2009. Measurement of the torque on a single stretched and twisted DNA using magnetic tweezers. *Phys. Rev. Lett.* 102:078301

70. Mosconi F, Allemand JF, Croquette V. 2011. Soft magnetic tweezers: a proof of principle. *Rev. Sci. Instrum.* 82:034302–12

71. Neuman KC, Block SM. 2004. Optical trapping. *Rev. Sci. Instrum.* 75:2787–809

72. Neuman KC, Lionnet T, Allemand JF. 2007. Single-molecule micromanipulation techniques. *Annu. Rev. Mater. Res.* 37:33–67

73. Neuman KC, Nagy A. 2008. Single-molecule force spectroscopy: optical tweezers, magnetic tweezers and atomic force microscopy. *Nat. Methods* 5:491–505

74. Noom MC, van den Broek B, van Mameren J, Wuite GJL. 2007. Visualizing single DNA-bound proteins using DNA as a scanning probe. *Nat. Methods* 4:1031–36

75. Otto O, Czerwinski F, Gornall JL, Stober G, Oddershede LB, et al. 2010. Real-time particle tracking at 10,000 fps using optical fiber illumination. *Opt. Express* 18:22722–33

76. Otto O, Gutsche C, Kremer F, Keyser UF. 2008. Optical tweezers with 2.5 kHz bandwidth video detection for single-colloid electrophoresis. *Rev. Sci. Instrum.* 79:023710

77. Ramanathan SP, van Aelst K, Sears A, Peakman LJ, Diffin FM, et al. 2009. Type III restriction enzymes communicate in 1D without looping between their target sites. *Proc. Natl. Acad. Sci. USA* 106:1748–53

78. Revyakin A, Ebright RH, Strick TR. 2004. Promoter unwinding and promoter clearance by RNA polymerase: detection by single-molecule DNA nanomanipulation. *Proc. Natl. Acad. Sci. USA* 101:4776–80

79. Revyakin A, Liu C, Ebright RH, Strick TR. 2006. Abortive initiation and productive initiation by RNA polymerase involve DNA scrunching. *Science* 314:1139–43

80. Ribeck N, Saleh OA. 2008. **Multiplexed single-molecule measurements with magnetic tweezers.** *Rev. Sci. Instrum.* 79:094301

81. Shroff H, Reinhard BM, Siu M, Agarwal H, Spakowitz A, Liphardt J. 2005. Biocompatible force sensor with optical readout and dimensions of 6 nm³. *Nano Lett.* 5:1509–14

82. Smith S, Finzi L, Bustamante C. 1992. **Direct mechanical measurements of the elasticity of single DNA molecules by using magnetic beads.** *Science* 258:1122–26

83. Strick T. 1999. *Mechanical supercoiling of DNA and its relaxation by topoisomerases*. PhD diss. Ecole Normal Supérieure, Paris

84. Strick T, Allemand J-F, Croquette V, Bensimon D. 2000. Twisting and stretching single DNA molecules. *Prog. Biophys. Mol. Biol.* 74:115–40

85. Strick TR, Allemand J-F, Bensimon D, Bensimon A, Croquette V. 1996. **The elasticity of a single supercoiled DNA molecule.** *Science* 271:1835–37

86. Strick TR, Allemand JF, Bensimon D, Croquette V. 1998. Behavior of supercoiled DNA. *Biophys. J.* 74:2016–28

87. Strick TR, Bensimon D, Croquette V. 1999. Micro-mechanical measurement of the torsional modulus of DNA. *Genetica* 106:57–62

88. Strick TR, Dessinges MN, Charvin G, Dekker NH, Allemand JF, et al. 2003. **Stretching of macromolecules and proteins.** *Rep. Prog. Phys.* 66:1–45

89. Taekjip H. 2001. Single-molecule fluorescence resonance energy transfer. *Methods* 25:78–86

90. te Velthuis AJW, Kerssemakers JWJ, Lipfert J, Dekker NH. 2010. Quantitative guidelines for force calibration through spectral analysis of magnetic tweezers data. *Biophys. J.* 99:1292–302

91. Towrie M, Botchway SW, Clark A, Freeman E, Halsall R, et al. 2009. Dynamic position and force measurement for multiple optically trapped particles using a high-speed active pixel sensor. *Rev. Sci. Instrum.* 80:103704–5

92. van Aelst K, Tóth J, Ramanathan SP, Schwarz FW, Seidel R, Szczelkun MD. 2010. Type III restriction enzymes cleave DNA by long-range interaction between sites in both head-to-head and tail-to-tail inverted repeat. *Proc. Natl. Acad. Sci. USA* 107:9123–28

93. van der Heijden T, Modesti M, Hage S, Kanaar R, Wyman C, Dekker C. 2008. Homologous recombination in real time: DNA strand exchange by RecA. *Mol. Cell* 30:530–38

94. van der Heijden T, Seidel R, Modesti M, Kanaar R, Wyman C, Dekker C. 2007. Real-time assembly and disassembly of human RAD51 filaments on individual DNA molecules. *Nucleic Acids Res.* 35:5646–57

80. First demonstration of parallel single-molecule magnetic tweezers.

82. First demonstration of single-molecule manipulation using magnetic tweezers.

85. First demonstration of supercoiling of a single dsDNA using magnetic tweezers.

88. Comprehensive review of the principle of magnetic tweezers and mechanical properties of DNA.

95. van der Heijden T, van Noort J, van Leest H, Kanaar R, Wyman C, et al. 2005. Torque-limited RecA polymerization on dsDNA. *Nucleic Acids Res.* 33:2099–105
96. van der Horst A, Forde NR. 2008. Calibration of dynamic holographic optical tweezers for force measurements on biomaterials. *Opt. Express* 16:20987–1003
97. van Loenhout MTJ, van der Heijden T, Kanaar R, Wyman C, Dekker C. 2009. Dynamics of RecA filaments on single-stranded DNA. *Nucleic Acids Res.* 37:4089–99
98. van Mameren J, Peterman EJG, Wuite GJL. 2008. See me, feel me: methods to concurrently visualize and manipulate single DNA molecules and associated proteins. *Nucleic Acids Res.* 36:4381–89
99. Vilfan ID, Lipfert J, Koster DA, Lemay SG, Dekker NH. 2009. Magnetic tweezers for single-molecule experiments. In *Handbook of Single-Molecule Biophysics*, ed. P Hinterdorfer, A van Oijen, pp. 371–95. New York: Springer
100. Wang Y, Shyy JY-J, Chien S. 2008. Fluorescence proteins, live-cell imaging, and mechanobiology: seeing is believing. *Annu. Rev. Biomed. Eng.* 10:1–38
101. Wong WP, Halvorsen K. 2006. The effect of integration time on fluctuation measurements: calibrating an optical trap in the presence of motion blur. *Opt. Express* 14:12517–31
102. Xiao B, Johnson RC, Marko JF. 2010. Modulation of HU-DNA interactions by salt concentration and applied force. *Nucleic Acids Res.* 38:6176–85
103. Yan J, Skoko D, Marko JF. 2004. Near-field-magnetic-tweezer manipulation of single DNA molecules. *Phys. Rev. E* 70:011905
104. Zhang H, Marko JF. 2008. Maxwell relations for single-DNA experiments: monitoring protein binding and double-helix torque with force-extension measurements. *Phys. Rev. E* 77:031916